9.

Effects of MR based attenuation correction on clinical interpretation and quantification of [^{18}F]flutemetamol scans: A comparison between PET/CT and PET/MR

S.M. Adriaanse, M. Yaqub, M.D. Zwan, P. Scheltens, F. Barkhof, A.A. Lammertsma, R. Boellaard, B.N.M. van Berckel

Submitted.

Abstract

Purpose [^{18}F]Flutemetamol (FMM) binds to amyloid-β, which is enhanced in Alzheimer's disease (AD). Recently, PET/MR systems have become available enabling acquisition of MR and human amyloid images in a single scanning session. PET/MR systems use MR based attenuation correction (MR-AC), which does not include actual attenuation coefficients, but rather uses tissue segmentation with allocation of standard attenuation coefficients to different tissue classes. This might result in bias, because bone cannot be segmented using a standard MR image. The aim of this pilot study was to assess the effects of MR-AC on clinical interpretation and regional distribution of FMM uptake.

Methods Ten memory-clinic patients underwent a PET/CT FMM scan, followed by a PET/MR scan. Regional standardized uptake value (SUV) and SUV ratios (SUVr), with cerebellar grey matter as reference, were calculated for all FMM scans. FMM SUVr scans were rated visually (amyloid-positive/amyloid-negative). PET/CT and PET/MR derived regional FMM SUVr were compared with each other.

Results Scans of 2 subjects were excluded due to movement and poor quality. Visual rating showed good agreement (7/8). Regional SUVr showed good correlation between PET/CT and PET/MR (r=0.93), although PET/MR values were higher than corresponding PET/CT values (mean 6.1%). This could be due to differences in AC or differences in scan time.

Conclusions PET/MR seems promising for routine clinical amyloid imaging, as it is patient friendly. Quantification of FMM SUVr on PET/MR should be explored further.

Introduction

Amyloid-β plaques are associated with Alzheimer's disease (AD) pathology [1]. Carbon-11 labelled Pittsburgh compound B ([^{11}C]PIB) was one of the first positron emission tomography (PET) tracers available for *in vivo* visualization of amyloid-β and it still is the most commonly used amyloid tracer in AD research. Recently, fluorine-18 labelled amyloid tracers have become available, making more widespread use of amyloid imaging possible. In the present study [^{18}F]flutemetamol (FMM) was used, but other tracers are also available [2].

Recently, PET/MR systems have become available enabling acquisition of both MR and amyloid images in a single scanning session, which is patient friendly [3]. In general, however, PET/CT systems are used for FMM imaging. In those systems the CT scan is used for attenuation correction (AC), which is essential for accurate quantitative measurements of radiotracer concentrations [4]. In case of PET/MR systems, attenuation correction is based on MR images (MR-AC), but these do not contain actual attenuation coefficients. Therefore, tissue segmentation is used followed by allocation of standard attenuation coefficients to different tissue classes [5]. This might result in bias, as bone cannot be segmented using a standard MR image and often air is not recognized by segmentation algorithms [6]. In addition, misalignment of the template used to correct for attenuation by the MR head coil can introduce bias [4].

Although bias in quantitative measurements of FMM is likely, it is not known whether this will affect actual clinical interpretation. The aim of the present pilot study was to assess the effects of MR-AC on clinical interpretation of FMM images by comparing PET/MR results with those obtained using a compatible PET/CT scanner.

Methods

Participants

Ten patients, part of the Amsterdam Dementia Cohort, were scheduled for FMM PET/CT examinations and asked to participate in this study. All participants received a standard dementia screening [7]. The study was approved by the Medical Ethics Review Committee of the VU University Medical Center. Written informed consent was obtained from the patients themselves and/or from their caregivers after complete written and verbal description of the study.

PET/CT and PET/MR FMM protocol

Patients received a bolus injection of 191±10 MBq FMM. Ninety minutes after injection, they underwent a low-dose CT scan followed by a 20 minutes (4x5 minutes) PET emission scan on a Gemini TF-64 PET/CT scanner (Philips Medical Systems, Best, the Netherlands) [8]. After this PET/CT scan and without a further FMM injection,

patients were scanned in a similar fashion (4x5 minutes frames) on a 3.0 Tesla Ingenuity TF PET/MR scanner (Philips Medical Systems, Cleveland, Ohio, USA). PET/MR scans were performed 137±2 minutes after injection of FMM. The PET/CT and PET/MR scanners used are based on similar PET hardware and reconstruction software, although for PET/MR some modifications have been implemented because of the combination with MR [3]. According to normal procedures, AC for PET/CT was based on the low-dose CT scan by scaling measured CT attenuation. For PET/MR standard predetermined attenuation coefficients were assigned to different tissue classes. For this purpose a special MR sequence (μ-map) was used and segmented in two tissue classes (air and soft-tissue) [5]. An MR coil (SENSE-Head-8) was used during the PET/MR FMM scan. A template was used to correct for attenuation by the coil [3]. All PET data were acquired in (dynamic) brain mode, using a sinogram based reconstruction algorithm (LOR-RAMLA). This resulted in a final voxel size of 2x2x2 mm^3 and a spatial resolution of 5-7 mm full width at half maximum.

Structural MR

Coronal T1-weighted 3-dimensional magnetization-prepared rapid-acquisition gradient echo (MPRAGE) images (voxel size 1×1×1mm^3) were acquired on the MR part of the PET/MR scanner.

PET analysis

Standardized uptake value (SUV) images, adjusted for injected mass and body weight were obtained for all FMM scans. Structural T1 images were aligned to corresponding PET images using a mutual information algorithm. PVE-lab, a software program with predefined regions of interest (ROIs) including cerebellum [7], was used to calculate SUV ratio (SUVr) [1]. FMM SUVr images were rated visually (amyloid-positive vs. amyloid-negative) by an expert reader who was blinded to subject and actual PET system used. FMM ratio images of both SUV and SUVr were obtained by dividing, on a voxel by voxel basis, PET/MR SUV and SUVr images by corresponding PET/CT images.

Statistical analysis

Regional SUVr for all PVE-lab regions (except ventricles, brainstem and cerebellum), were averaged over left and right regions, resulting in data for 29 ROIs. Pearson correlation of FMM SUVr on PET/CT and PET/MR was calculated within subjects and ROIs. The percentage overestimation of PET/MR SUVr compared to PET/CT for all ROIs was calculated and evaluated with a one-sample t-test.

Results

Data of 8 subjects were suitable for analysis (Table 1). Scans of 2 patients were excluded due to movement and a structural scan of poor quality. A representative example of positive FMM scans of the same patient acquired on both PET/CT and PET/MR scanners is shown in Figure 1.

Table 1: Subject demographics

N	8
Age	61 ± 8
Sex (M/F)	1/7
MMSE score	23 ± 4
Time between FMM injection and start PET/MR (minutes)	137 ± 2
Amyloid-positive PET/CT	6
Injected dose FMM (MBq)	191 ± 10
Average regional FMM SUVr amyloid-positive subjects (PET/CT – PET/MR)	1.76 – 1.92*
Average regional FMM SUVr amyloid-negative subjects (PET/CT – PET/MR)	1.24 – 1.29

Data are presented as mean ± standard deviation (SD). MMSE = Mini Mental State Examination. FMM = [18F]flutemetamol. The subject with different visual rating for PET/CT and PET/MR was included in this average (For this subject average FMM SUVr was 1.59 on PET/CT and 1.82 on PET/MR).

FIGURE 1: Example of corresponding FMM images that were rated as amyloid-positive on both PET/CT (top row) and PET/MR (bottom row). Data from this subject are representative for the entire sample.

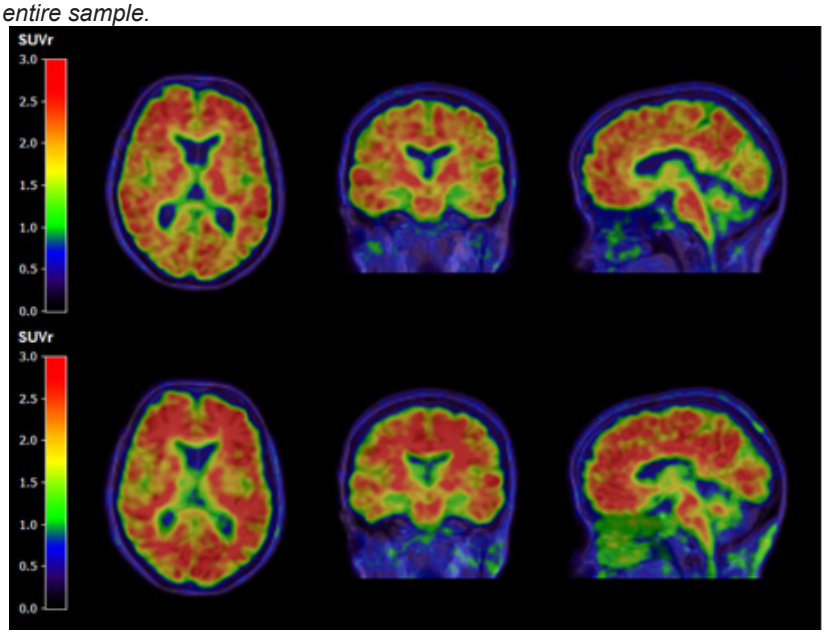

Visual rating

Visual rating showed agreement between PET/CT and PET/MR images for 7 of the 8 patients. Of the 8 FMM scans on PET/CT, 6 were rated as amyloid-positive. For FMM scans on PET/MR, 5 of the 8 subjects were rated as amyloid-positive. One scan that was rated as 'borderline' amyloid-positive on PET/CT was rated as amyloid-negative on PET/MR (Figure 2).

FIGURE 2: Subject with different visual ratings of FMM images on PET/CT (top row: amyloid-positive) and PET/MR (bottom row: amyloid-negative).

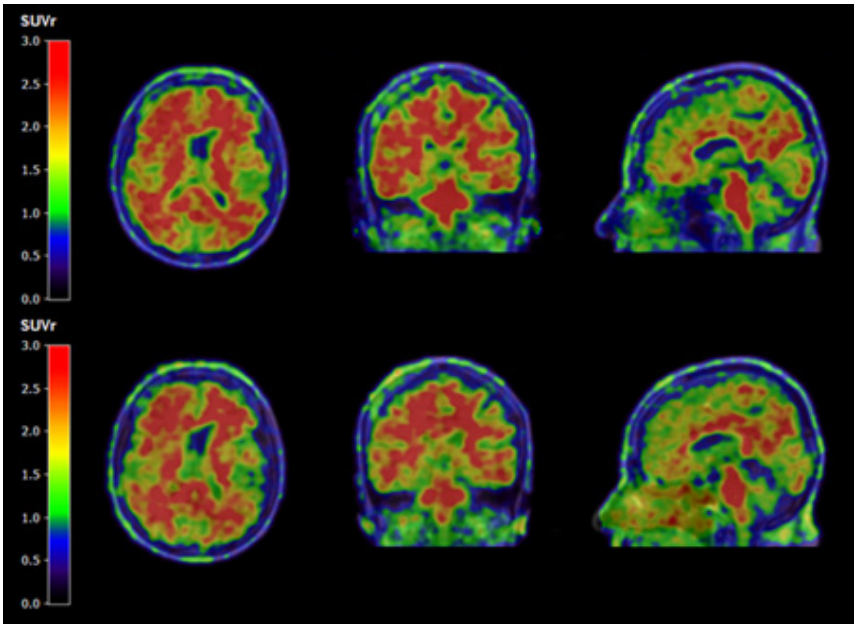

Regional SUVr

Overall, regional SUVr within subjects showed good correlation between PET/CT and PET/MR (Figure 3) with an average correlation of r=0.93 (range: 0.87-0.97). Average FMM SUVr for PET/CT and PET/MR are listed in Table 1. PET/MR SUVr was significantly higher than corresponding PET/CT SUVr with an average relative difference for all ROIs of 6.1±3.3% (range: 1.5-11.0%). Significantly higher PET/MR SUVr were seen in 20 of the 29 ROIs (Supplementary Table 1). The average regional correlation was r=0.92, with strong (≥r=0.90) correlations for 26 ROIs. Weak correlations were found for hippocampus (r=0.54), amygdala (r=0.52) and parahippocampal and ambient gyri (r=0.44).

FIGURE 3: Scatterplot of regional FMM SUVr measured using PET/CT and PET/MR across subjects. Different colours represent different subjects. The black line represents the line of identity.

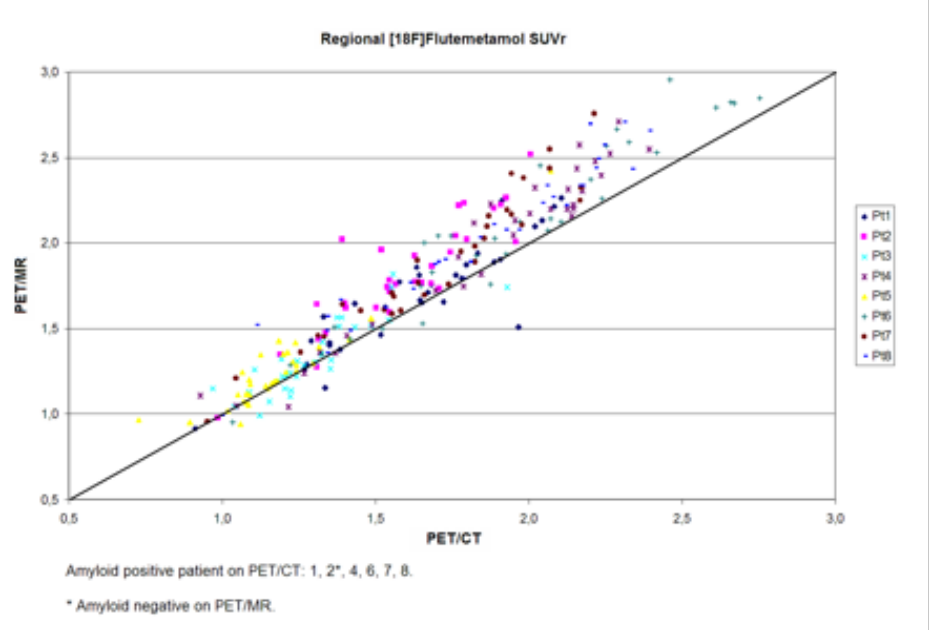

Ratio of FMM SUV and SUVr images

For PET/MR, an underestimation of FMM SUV in cortical regions close to skull was observed as compared with PET/CT, and an overestimation was seen in air-filled regions. In case of FMM SUVr ratio images, PET/MR appeared to show an overestimation in the centre of the brain (Figure 4).

FIGURE 4: A: Ratio of PET/MR and PET/CT derived FMM SUV images for an amyloid-negative (top images) and an amyloid-positive (bottom images) subject. B: Ratio of PET/MR and PET/CT derived FMM SUVr images for the same subjects. Images were smoothed with a Gaussian Kernel of 5 mm full width at half maximum. The black line represents the outline of the structural MRI.

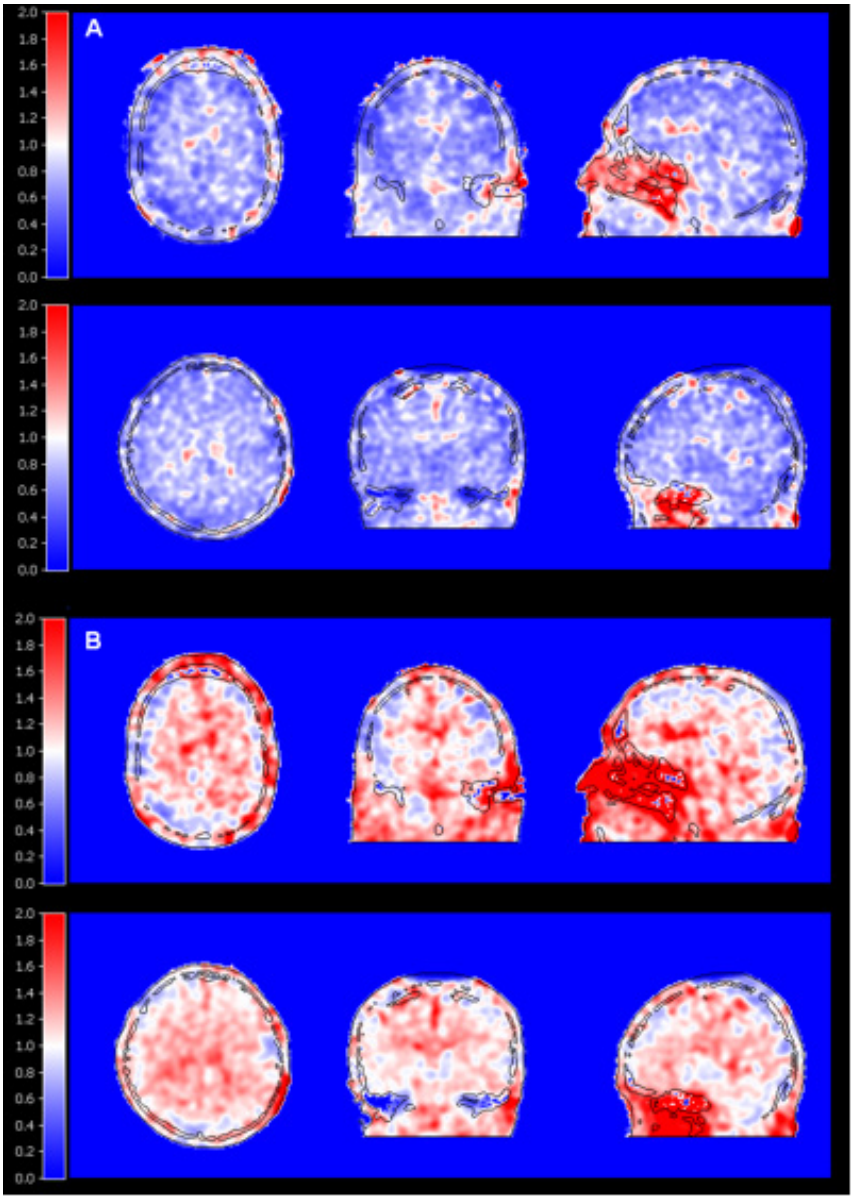

Discussion

To the best of our knowledge this is the first study describing sequential acquisition of amyloid scans on PET/CT and PET/MR scanners with similar PET hardware and reconstruction software. Overall, visual inspection of FMM scans on PET/CT and PET/MR showed good agreement. Regional SUVr strongly correlated between PET/CT and PET/MR, although SUVr on PET/MR was higher.

Visual rating of FMM images was in agreement for 7 of the 8 subjects. One subject changed from amyloid-positive on PET/CT to amyloid-negative on PET/MR, which is could be due to differences in AC or scan time between the two modalities. It should be noted, however, that the PET/CT FMM scan for this subject was rated as borderline positive. This was in line with both average FMM SUVr for this subject and amyloid-β level in cerebral spinal fluid (CSF).

As mentioned above, no perfect solution is available for MR-AC yet. MR-AC in the present study was based on simple tissue segmentation and therefore ignores skull [6]. Alternatives do exist, such as population based atlases, use of CT information, ultra-fast MR-sequences for bone visualization and dedicated reconstruction methods [9], but these have not been incorporated into routine PET/MR yet [10]. Especially at the edges of the brain, PET/MR is reported to underestimate the signal by up to 25% [6]. Overall, regional SUVr was significantly higher for PET/MR than for PET/CT. This might seem counterintuitive but is due to lower apparent uptake of FMM on PET/MR. Underestimation of SUV on PET/MR was seen throughout the entire brain. This was most pronounced in brain regions close to skull, such as the cerebellum, since these are more vulnerable to AC effects [6]. Using an underestimated signal as reference will cancel out the underestimation of the signal in cortical regions. This will also result in overestimation in regions located in the centre of the brain since they are less vulnerable to the initial bias of MR-AC [4;6]. This might explain why the 5 ROIs with 10% higher PET/MR than PET/CT SUVr were all located in the centre of the brain. Test-retest variability, in regions vulnerable for atrophy, could explain low regional correlations in hippocampus, amygdala and parahippocampal gyri [7].

Alternatively, the different time windows of PET/CT and PET/MR scans could have resulted in different contrast between cortex and reference region. Nevertheless, the PET/MR scan was still performed within the optimal time window (80-170 minutes post-injection, the ratio of neocortical to cerebellar uptake is maximal and stable) for acquisition of FMM [1]. Random assignment of PET/CT or PET/MR as first scan would have been preferable, but not possible since PET/CT FMM was used for clinical purposes.

In conclusion, PET/MR seems to hold promise for routine clinical amyloid imaging. Future studies should focus on quantification of amyloid binding. For this purpose, an additional injection of FMM for PET/MR and a dynamic scanning protocol are necessary. Ideally, those studies should consist of an even distribution of amyloid-positive and amyloid-negative scans.

Disclosure

The VUmc Alzheimer center is supported by Alzheimer Nederland, Stichting VUmc Fonds and Stichting Diorapthe. The department of Radiology and Nuclear Medicine of the VUmc has a research collaboration with Philips Healthcare. No other potential conflicts of interest relevant to this article are reported.

Ethics statement

The study was approved by the Medical Ethics Review Committee of the VU University Medical Center. Ethics review criteria conformed to the Helsinki declaration 2013. Written informed consent was obtained from patients and/or their caregivers after complete written and verbal description of the study.

Supplementary information

Table 2: Overview of the 20 ROIs showing significant different SUVr (from 0%) values on PET/MR compared with PET/CT. Total number of ROIs was 29.

	Δ SUVr	p-value
Posterior cingulate cortex	14.9%	<0.001
Anterior cingulate cortex	14.6%	<0.001
Lingual gyrus	14.5%	<0.001
Gyrus rectus	14.1%	<0.001
Nucleus accumbens	10.0%	0.003
Superior frontal gyrus	9.3%	<0.001
Superior parietal gyrus	8.9%	0.001
Orbifrontal gyrus	8.1%	0.009
Parahippocampal and ambient gyri	7.3%	0.030
Caudate nucleus	6.7%	0.003
Postcentral gyrus	6.2%	0.005
Cuneus	6.2%	0.015
Precentral gyrus	5.9%	0.003
Posterior temporal lobe	5.5%	0.005
Putamen	5.1%	0.021
Insula	5.1%	0.032
Lateral remainder of occipital lobe	4.6%	0.003
Inferior frontal gyrus	4.0%	0.005
Superior temporal gyrus	3.6%	0.029
Anterior temporal lobe lateral part	-6.5%	0.027

Δ SUVr = percentage overestimation PET/MR SUVr compared to PET/CT SUVr

References

[1] Nelissen N, Van Laere K, Thurfjell L, et al. Phase 1 study of the Pittsburgh compound B derivative 18F-flutemetamol in healthy volunteers and patients with probable Alzheimer disease. J Nucl Med. 2009;50:1251-1259.

[2] Koole M, Lewis, D, Buckley C. Whole-body biodistribution and radiation dosimetry of 18F-GE067: A radioligand for in vivo brain amyloid imaging. J Nucl Med. 2009;50:818-22

[3] Zaidi H, Ojha N, Morich M, et al. Design and performance evaluation of a whole-body Ingenuity TF PET-MRI system. Phys Med Biol. 2011;56:3091-3106.

[4] Catana C, van der Kouwe A, Benner T, et al. Toward implementing an MRI-based PET attenuation-correction method for neurologic studies on the MR-PET brain prototype. J Nucl Med. 2010;51:1431-1438.

[5] Martinez-Moller A, Souvatzoglou M, Delso G, et al. Tissue classification as a potential approach for attenuation correction in whole-body PET/MRI: evaluation with PET/CT data. J Nucl Med. 2009;50:520-526.

[6] Andersen F, Ladefoged C, Beyer T, et al. Combined PET/MR imaging in neurology: MR-based attenuation correction implies a strong spatial bias when ignoring bone. Neuroimage. 2014;84:206-216.

[7] Ossenkoppele R, Tolboom N, Foster-Dingley J, et al. Longitudinal imaging of Alzheimer pathology using [11C]PIB, [18F]FDDNP and [18F]FDG PET. Eur J Nucl Med Mol Imaging. 2012;39:990-1000.

[8] Surti S, Kuhn A, Werner M, Perkins AE, Kolthammer J, Karp JS. Performance of Philips Gemini TF PET/CT scanner with special consideration for its time-of-flight imaging capabilities. J Nucl Med. 2007;48:471-480.

[9] Boellaard R, Hofman MBM, Hoekstra OS, Lammertsma AA. Accurate PET/MR quantification using time of flight MLAA image reconstruction. Mol Imaging Biol. 2014; 16:469-477.

[10] Bailey D, Barthel H, Beuthin-Baumann B, et al. Combined PET/MR: Where are we now? Summary report of the second international workshop on PET/MR imaging April 8-12, 2013, Tubingen, Germany. Mol Imaging Biol. 2014;16:295-310.